European Journal of Nuclear Medicine and Molecular Imaging
https://doi.org/10.1007/s00259-019-04545-8

ORIGINAL ARTICLE

Dynamic patterns of [^{68}Ga]Ga-PSMA-11 uptake in recurrent prostate cancer lesions

Ian Alberts[1] · Christos Sachpekidis[1] · Eleni Gourni[1] · Silvan Boxler[2] · Tobias Gross[2] · George Thalmann[2] · Kambiz Rahbar[3] · Axel Rominger[1] · Ali Afshar-Oromieh[1]

Received: 9 July 2019 / Accepted: 20 September 2019

Abstract

Purpose Dual-time point PET/CT scanning with [^{68}Ga]Ga-PSMA-11 in the diagnosis of prostate cancer (PC) has been advanced as a method to increase detection of PC lesions, particularly at early stages of biochemical recurrence and as a potential means to aid the discrimination between benign and pathological prostate-specific membrane antigen (PSMA) uptake. However, the assumption that all PC lesions uniformly exhibit increasing tracer uptake at delayed imaging has not yet been investigated, which this present study aims to address.

Methods One hundred consecutive patients with biochemically recurrent PC who received standard and late [^{68}Ga]Ga-PSMA-11 PET/CT (by local protocol at 1.5 h "standard" and 2.5 h p.i. "late") underwent retrospective evaluation. All lesions with a tracer uptake above local background were analysed with regard to their maximum standardised uptake values at standard and late images (SUVmax) and characterised according to their morphological characteristics.

Results Seventy-nine of 100 patients had PSMA-positive scans, in whom a total of 185 individual PSMA-positive lesions were identified. These were morphologically characterised as bone lesions (n = 48), solid organ lesions (n = 3), lymph node (LN) lesions (n = 78) and locally recurrent lesions in the prostatic fossa or seminal vesicles (n = 56). The relative uptake between standard and late imaging was considered; all lesions classified as local recurrence presented with increasing (86%) or stable patterns of tracer uptake (14%). In contrast, only 58% of bone lesions exhibited increasing tracer uptake, with 21% exhibiting a stable pattern and 21% exhibiting a decreasing tracer uptake at late imaging.

Conclusion A heterogeneous pattern of dynamic tracer uptake was observed, with a largely increasing pattern observed for locally recurrent lesions and lymph nodes and a significant proportion of bone lesions exhibiting decreasing tracer uptake. The results are of significance not only in the imaging and identification of PC lesions, but they also have implications for PSMA-directed ligand therapy.

Keywords Prostate cancer · PET/CT · Positron emission tomography · PSMA · Prostate-specific membrane antigen · Ganglion

Introduction

Prostate cancer (PC) is the most common malignancy in men, and the third leading cause of cancer-related death in men [1]. Despite initial therapy at early-stage disease, biochemical recurrence remains a commonly encountered entity and presents a challenge for conventional imaging modalities given their limited abilities to detect disease at early stages of recurrence. Although the exact timing of salvage radiotherapy (SRT) remains a topic of debate, early SRT may be beneficial for some patients [2].

The prostate-specific membrane antigen (PSMA) has become the focus of much attention owing to its high levels of expression on PC cells [3] and has rapidly established itself as

This article is part of the Topical Collection on Oncology – Genitourinary

Electronic supplementary material The online version of this article (https://doi.org/10.1007/s00259-019-04545-8) contains supplementary material, which is available to authorized users.

✉ Ian Alberts
ian.alberts@insel.ch

[1] Department of Nuclear Medicine, Inselspital, Bern University Hospital, University of Bern, Freiburgstr. 18 3010 Bern Switzerland

[2] Department of Urology, Inselspital, Bern University Hospital, University of Bern, Bern Switzerland

[3] Department of Nuclear Medicine, University Hospital Münster, Münster Germany

Published online: 18 October 2019

the investigation of choice in recurrent PC [4–7]. Furthermore, PSMA-directed radioligand therapy is a rapidly evolving treatment modality for metastatic disease, creating an additional theragnostic role for PSMA ligand molecular imaging [8]. However, previous studies have demonstrated that at PSA values of less than 0.2 ng/mL, the diagnostic performance of PSMA ligands remains limited [5]. The challenge for nuclear medicine is therefore to develop tracers and examination protocols suitable at the early stages of recurrence.

Another challenge for PSMA ligand imaging is specificity. Despite its name, PSMA expression is not limited to PC cells, but is observed in a wide variety of pathological and physiological tissues. For example, it has been demonstrated that PSMA is expressed by the neovasculature of a wide variety of solid tumours [9]. Physiological PSMA expression is reported in the lacrimal and salivary glands, the liver, the spleen, the kidneys and the intestines [10]. PSMA ligand uptake has also been observed in benign mediastinal lymph nodes, creating a potential pitfall when interpreting images [11]. Furthermore, numerous publications have demonstrated PSMA-avid peripheral nerve ganglia [12–16], presenting a second potential pitfall for the unaware or inexperienced reader.

Given these circumstances, the observation that, owing to increased tracer uptake at late imaging, the detectability of PC lesions is increased with dual-time point scanning is of significance for imaging protocols at early stages of recurrence [17]. Furthermore, when faced with the challenge of interpreting a PSMA-avid lesion and in the discrimination between benign but PSMA-avid structures such as ganglia and pathological lesions of PC, dynamic patterns of tracer uptake may provide the reader with additional diagnostic data. However, despite (at the time of writing) 8 years of routine clinical use, the dynamic patterns of tracer uptake have not yet been published for each individual lesion type, which this present study aims to address.

Materials and methods

In this retrospective analysis, we investigated 100 individuals (characteristics outlined in Table 1) with biochemically recurrent PC who were referred to our centre for [^{68}Ga]Ga-PSMA-11 PET/CT between August 2018 and March 2019. Since numerous publications have shown the advantages of later scanning in PSMA imaging [10, 17–19], clinical routine at our centre is to perform additional late imaging at 2.5 h p.i. (with standard imaging at 1.5 h p.i.) in cases of indeterminate findings at standard imaging or to increase the probability of tumour detection in cases of negative standard scans. Due to the retrospective nature of the analysis, it is not possible to reconstruct the particular situations in which the decision was made to conduct an additional late scan.

Details regarding age, Gleason score, initial staging, applied activity and the prostate-specific antigen (PSA) value at the time of scanning are as outlined in Table 1.

Radiotracer

[^{68}Ga]Ga-PSMA-11 was produced as previously described [7, 20] and was given by intravenous bolus injection (mean of 202 ± 35 MBq, range 124–280 MBq).

Imaging

All patients received regular whole-body PET scans (from head to the thighs) at 1.5 h p.i. following oral hydration with 1 L of water (beginning from 30 min p.i.) and 20 mg of i.v. furosemide (at 1 h p.i.). Late imaging was performed at 2.5 h p.i. (from xiphoid process to thighs, and additionally head/neck for one individual) with oral hydration ad libitum. Both scans at 1.5 h and 2.5 h p.i. were analysed for pathological lesions characteristic for PC.

Table 1 Patient characteristics

Characteristic	Values
Age (mean/standard deviation/range/median)	68/6.7/48–89/69
Gleason score (frequency in %)	6 (8%); 7 (59%); 9 (29%); 10 (1%)
PSA (ng/mL) (mean/standard deviation/range/median)	9/28.8/0.33–193/1.1
Initial therapy	70 × OP
	11 × OP + RT
	2 × chemo
	10 × RT
Initial TNM	T: 3 × T1, 28 × T2, 54 × T3, 1 × T4
	N: 18 × N1
	M: 2 × M1
Injected activity (MBq) (mean/standard deviation/range/median)	213/32/124–335/204

PSA, prostate-specific antigen; *OP*, operative treatment; *RT*, radiotherapy

Image acquisition

All patients were investigated using either a Biograph VISION-600 PET/CT digital scanner (n = 65) or one of two cross-calibrated Biograph-mCT PET/CT scanners (Siemens, Erlangen, Germany) (n = 35). Both sets of images were acquired on the same scanner for each individual. The details of the imaging protocol, which due to the varying performance of the two scanner types differed, can be found in the supplementary materials.

Image evaluation

Image analysis was performed using an appropriate workstation and software (SyngoVia; Siemens, Erlangen, Germany). Two experienced physicians (one post-graduate physician with 7 years of clinical experience and one board-certified nuclear physician with 14 years of experience—first and last authors, respectively) read all data sets together and resolved any disagreements by consensus. Lesions that were visually considered as suggestive for PC exhibiting increased tracer uptake relative to local background and located within the field of view of both sets of imaging (standard and late) were counted and analysed with respect to their type (local relapses, lymph node, bones, solid organ), to their localisation and to their maximum standardised uptake value (SUVmax) for the standard and late images. The lesions identified by consensus as benign structures such as ganglia, ureteric tracer uptake or non-specific tracer uptake associated with clearly identifiable structures such as bone fractures were disregarded for the purposes of this study, as were the areas of increased uptake without clear computer tomographic (CT) correlates, as described previously [21]. Visual criteria for the differentiation between ganglia and lymph nodes were as described previously [16] and aided by a co-registered thin-slice CT (1 mm).

For the calculation of the SUVmax, circular regions of interest were drawn around areas with focally increased uptake in transaxial slices and automatically adapted to a three-dimensional volume of interest at a 40% isocontour as previously described [7]. Cross-sectional dimension (x- and y-axis) for each lesion was measured from the co-registered CT.

The measurement of the SUVmax at 1.5 h and 2.5 h allowed for a percentage change in tracer uptake to be obtained. The percentage changes between − 10 and + 10% were considered to be "stable", i.e. showing no significant change. Those greater than + 10% were considered to be "increasing" and those less than − 10% were considered to be "decreasing". Ten percent is a conservative estimate based on previously reported variability in the SUV measurements [22, 23]. Cognisant of the influence of scanner type and reconstruction algorithm, we restricted a subsequent statistical analysis to the dimensionless ratio of early to late tracer uptake, thereby considering patterns of change only rather than absolute SUVmax, which cannot be directly compared between scanner types.

Statistical analysis

The SUVmax values of the PC lesions at 1.5 h and 2.5 h p.i. were compared using the paired two-tailed Student's t test to evaluate the differences between the standard and late images and the unpaired t test to evaluate the differences between lesion types; a two-tailed p value of < 0.05 was considered statistically significant.

A regression analysis was performed to interrogate possible relationships between the lesion size and patterns of tracer uptake, with calculation of the R^2 value. The univariate analysis of variance (ANOVA) was performed to interrogate potential variations in cross-sectional diameter and lesion behaviour. Unpaired, two-tailed Student's t test tested potential differences for each lesion type by scanner type. All statistical tests were performed in Excel (Microsoft, Redmond, WA, USA).

Results

PC lesions

In our cohort of 100 patients, a total of 185 lesions of PC were identified in 79 patients. We note that an extra 15 lesions were noted for 13 patients at 2.5 h compared with those at 1.5 h, which resulted in a clinically relevant stage change for 5 patients.

As outlined in Table 2, the lesions were morphologically characterised as bone (n = 48), solid organ (n = 3), lymph node (LN) (n = 78) and locally recurrent lesions in the prostatic fossa or seminal vesicles (n = 56).

Lesion uptake

The SUVmax at 2.5 h was significantly higher ($p < 0.05$) than at 1.5 h for bone, LN and locally recurrent lesions. No change ($p = 0.94$) was observed for the solid lesions; however, this is based on three lesions in one individual, all of which were liver lesions.

Table 2 Number of lesion types identified

Lesion type	Number (n)	Number (%)
Bone	48	26
Liver	3	2
Lymph node	78	42
Local recurrence	56	30
Total	185	

Patterns of tracer uptake

Comparing SUVmax at 1.5 h and at 2.5 h, a dynamic pattern of uptake and a percentage change in SUVmax can be identified. We grouped all lesions by "increasing" (percentage increase greater than 10%), "decreasing" (percentage decrease greater than − 10%) and "stable" (percentage change between − 10 and 10%). The results are shown in Fig. 1. We note that the majority of lesions exhibited increasing or stable patterns of tracer uptake: 86% of locally recurrent lesions exhibited increasing tracer uptake, and the remainder exhibiting a stable pattern. Likewise, 72% of LN exhibited increasing and 23% stable uptake, with only 5% showing decreasing tracer uptake. However, only 58% of bone lesions showed increasing uptake, with 21% exhibiting a falling uptake.

We observed patterns of concomitant increasing and decreasing uptake patterns in the same lesion type. For example, of the three solid organ (liver) metastases observed, two exhibited an increasing pattern and one decreasing pattern (in the same patient). Such discordant patterns of tracer behaviour were observed in five patients.

We present PET/CT image examples for a sample of lesion types and behaviours. Figure 2 shows a discordant response for PSMA-positive liver lesions. Figure 3 shows a decreasing tracer uptake at late imaging in a PSMA-positive bone lesion. Figure 4 shows an increasing tracer uptake at late imaging in a PSMA-positive lymph node.

Relationship with lesion size

The short- and long-axis (x, y) was measured from the co-registered CT images. Possible relationships between both tracer uptake (SUVmax) and patterns of behaviour were considered. Only a weak correlation between SUVmax and axis diameter (R^2 = 0.11) was observed and a weakly negative correlation between percentage change and axis diameter (R^2 = 0.095). Grouping the lesions by uptake behaviour (increasing, stable and decreasing), we note that 77% of both the increasing and stable group and 80% of the decreasing group had a cross-sectional diameter of less than 0.5 cm, i.e. no significantly increased frequency. ANOVA was performed for cross-sectional diameter grouped by lesions with increasing, stable and decreasing tracer uptake, with no significant difference in between-group variance.

Relationship with scanner type

The scanner type as a potential confounder was interrogated. No statistically significant differences in the percentage change ($p > 0.05$) were observed between the scanner for PSMA-avid lesions of the bone (p = 0.8), LN (p = 0.2) and locally recurrent PC (p = 0.2). Solid lesions were found in only one patient, meaning that no comparison for this lesion type was possible.

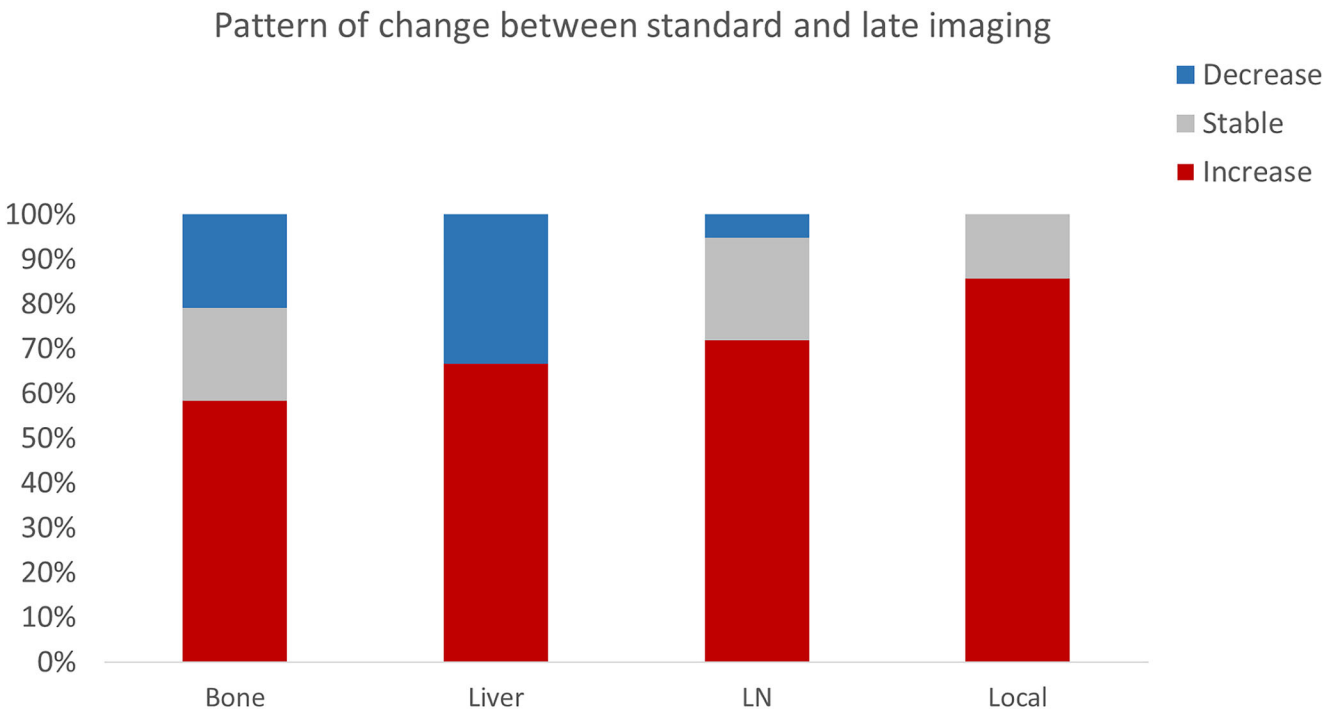

Fig. 1 The dynamic patterns of tracer uptake. Whereas the majority of locally recurrent lesions exhibited either increasing or stable patterns of tracer uptake, 5% of lymph node (LN) and 21% of bone lesions exhibited decreasing patterns of tracer uptake. The data for liver lesions are presented, however, with only n = 3 lesions no broad trends can be interpreted

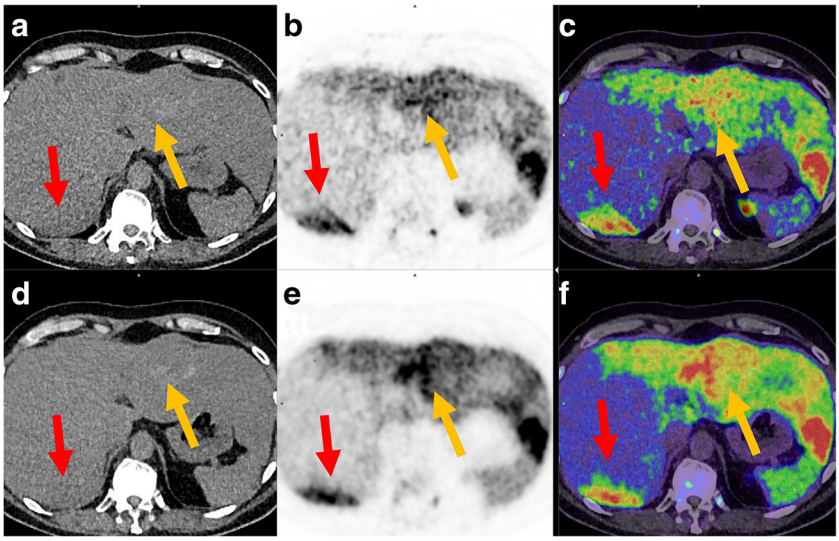

Fig. 2 An example showing discordant tracer uptake (top row, late imaging; bottom row, standard imaging). Whereas the lesion in the right lobe of the liver (yellow arrow) shows visual decrease in the late images (SUVmax standard 10.9, SUVmax late 9.1), the lesion in the right lobe of the liver shows moderate visual increase (red arrow; SUVmax standard 15.2, SUVmax late 16.9). The lesions have no clear CT correlate in the non-contrast-enhanced CT (left column, tiles **a** and **d**; soft-tissue window), but are clearly discernible in the PET (middle column, tiles **b** and **e**; PET window 0–10 SUV) and the fused PET/CT (right column, tiles **c** and **f**)

Discussion

Previous studies have demonstrated the limited diagnostic performance of PSMA ligand imaging at early stages of recurrence (i.e. low PSA values), including studies reporting data for both [^{68}Ga]Ga-PSMA-11 [5] and [^{18}F]F-PSMA-1007 [24]. To this end, the notion that PC lesions are generally associated with increasing tracer uptake at late (delayed) imaging is significant and is largely supported by our findings. In keeping with previous publications, we note that a higher number of lesions were visible at 2.5 h (15 lesions in 13 patients), which resulted in a change in clinical stage for 5 patients [17]. Late imaging is endorsed by the joint EANM/SNMMI guidelines for PET/CT with PSMA ligands for indeterminate scans at 60 min p.i. or low PSA values [25].

Nevertheless, despite excellent sensitivity, numerous studies have reported cases of unspecific PSMA expression, resulting in numerous diagnostic pitfalls for the unaware [26]. One such example is ganglia [12, 14]. Indeed, in a PET/MRI study of coeliac ganglia, Bialek and Malkowski reported that roughly 50% of patients presented with at least one coeliac ganglia which was confusable with a PSMA-positive lymph node either on grounds of size, shape or tracer uptake [27]. We expect that with new-generation digital PET/CT scanners reporting ever higher sensitivity and resolution [28], and reports of higher rates of artefactual tracer uptake

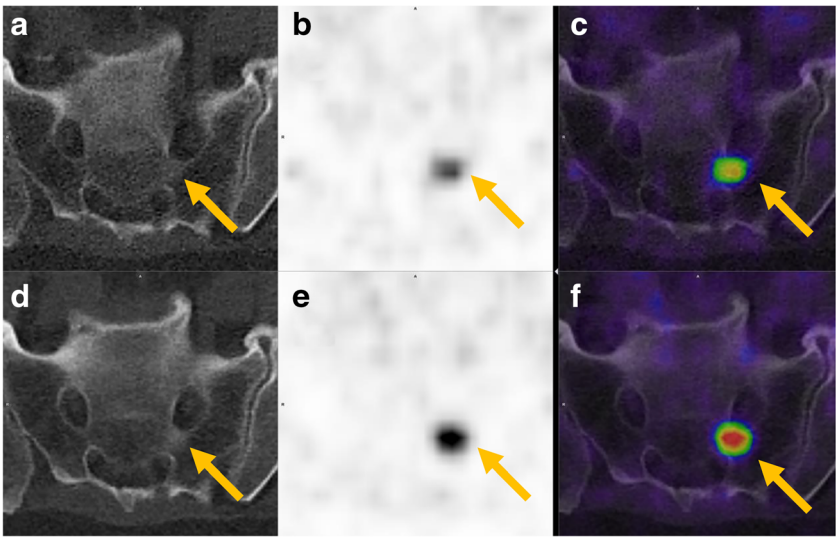

Fig. 3 An example showing decreasing tracer uptake in a sacral bone lesion (shown by arrow; SUVmax standard 15.7, SUVmax late 13.2). A clear visual decrease can be seen between the standard images (bottom row) and the late images (top row). Left column CT (bone window, tiles **a** and **d**), middle column PET (tiles **b** and **e**, PET window 0–10 SUV) and fused PET/CT (right column, tiles **c** and **f**)

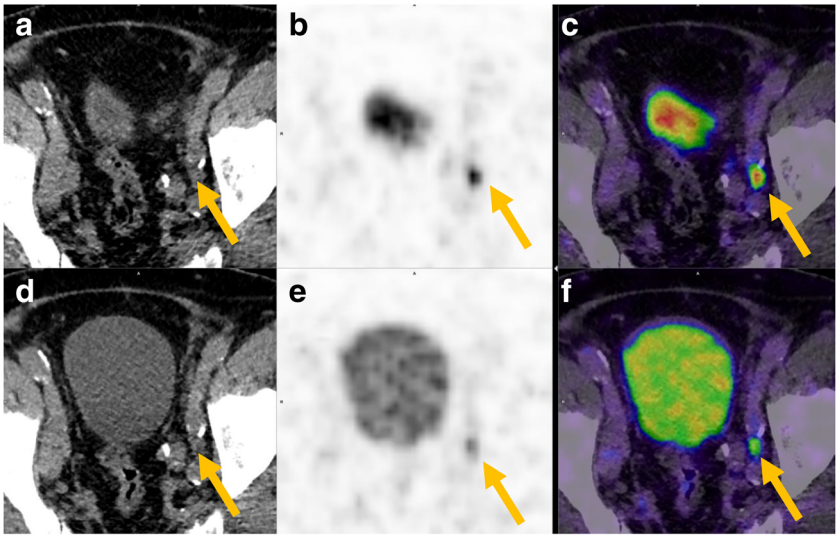

Fig. 4 An example of increasing tracer uptake in an inguinal lymph node. Although faintly discernible at standard imaging (bottom row), the lesion (shown by the arrow) is seen to increase its tracer uptake (SUVmax standard 5.3, SUVmax late 10.9) at late imaging (top row). Left column CT (soft-tissue window, tiles **a** and **d**), middle column PET (tiles **b** and **e**, PET window 0–10 SUV) and fused PET/CT (right column, tiles **c** and **f**). We note that without the PET image, the lymph node is discernible only with difficulty in the non-contrast CT

using 18F-labelled radioligands [29], this issue is likely to be of increasing importance. Given the observation that SUVmax increases at late imaging, patterns of tracer uptake might be reasonably supposed to provide additional diagnostic information regarding the likelihood of malignancy. However, to our knowledge, such dynamic tracer uptake patterns have not been reported for additional late imaging.

With this in mind, we sought to describe the dynamic patterns of tracer uptake for various lesion types. In our cohort of 100 patients, 79 patients presented with lesions which met our inclusion criteria (namely, present in both standard and late imaging which included the pelvis and abdomen only), a detection rate broadly in keeping with previously reported studies [30].

As was expected, we found that locally recurrent and LN lesions presented with predominantly increasing tracer uptake at late imaging, in agreement with previous reports [10, 17]. However, to our surprise, only 58% of bone lesions exhibited this characteristic, with 21% of such lesions demonstrating a greater than 10% fall in SUVmax at later imaging. Likewise, in a very small sample (only one patient exhibited solid organ metastasis), two solid (liver) lesions exhibited increasing tracer uptake and one decreasing tracer uptake. We cautiously interpret this single finding as also indicative that liver metastases can also exhibit heterogeneous uptake. The analysis of larger patient cohorts directed to this particular question is necessary to confirm this finding.

Whereas the physical half-life of the radioisotope (^{68}Ga) is short (68 min), previous studies have confirmed that [^{68}Ga]Ga-PSMA-11 exhibits an increase in tracer uptake over time in a majority of PC lesions [10, 11, 17, 26]. This increase is a result of high PSMA receptor expression, which is in turn highly correlated with malignancy [31], and it is this property which underlies the high clinical utility of PSMA ligands [10]. A number of studies have sought to demonstrate the pharmacokinetics of radiotracer uptake using early dynamic acquisition protocols. For example, Sachpekidis et al. report a two-tissue compartment model for radioligand distribution in the intravascular and interstitial space, reporting equilibrium constants for tracer binding to and dissociation from the PSMA receptor for primary PC lesions, lymph nodes and lesions of bone [32].

Following binding to the PSMA receptor, internalisation of the bound ligand and receptor occurs via clathrin-coated pits. Either the receptor can recycle back to the plasma membrane through the recycling endosomal compartment (REC) or endocytosis can occur through late endosomes. The direction of receptors to endocytic compartments and vesicular trafficking is directed by numerous signalling pathways, including the tyrosine-kinase pathway [33]. Budäus et al. hypothesise that an intense tracer uptake by highly PSMA-expressive lesions may reduce blood-pool tracer availability, thereby acting as a pharmacokinetic confounder for other more weakly expressive lesions [34]. Tracer uptake should therefore be regarded as the interaction of complex pharmacological factors such as radiotracer availability, internalisation and cell signalling as well as patterns of PSMA expression.

Considering these factors, we interpret our finding that nearly one in five bone lesions exhibited falling tracer uptake as pointing towards potentially important differences in, and heterogeneity of, bone metastases. Indeed, this is in keeping with the finding of Sachpekidis et al. of a significantly higher equilibrium constant of tracer binding and internalisation for bone compared with primary PC and LN lesions [32]. Interestingly in a subsequent study considering bone metastases, these kinetic parameters were observed to correlate with PSA values [21]. Furthermore, Wieser et al. report lower detection rates for bone metastases using the bombesin-targeted ligand [^{68}Ga]Ga-RM2 compared with [^{18}F]F-fluoroethylcholine PET [35], which was also confirmed by Mitsakis et al. using another bombesin-targeted ligand [^{68}Ga]Ga-NODAGA-MJ9 [36]. In both studies,

whereas bombesin tracer uptake was higher in lymph node and locally recurrent lesions compared with choline, tracer uptake was uniquely lower in bone lesions, pointing towards another important difference in the behaviour of bone metastases. This finding also finds support in initial clinical experience PSMA-directed radioligand therapy, with anecdotal reports describing bone lesions as responding less well than the other types of lesions. We eagerly anticipate the results of ongoing trials for ^{177}[Lu]Lu-PSMA-617 which may provide confirmation of this potentially significant finding [8]. However, encouraged by this plethora of data, we propose that PC bone lesions exhibit true differences in PSMA expression. Furthermore, we note that the assumption that increasing tracer uptake at late imaging is pathognomonic for malignancy is incorrect for bone lesions, representing a significant diagnostic pitfall that hitherto has received scant attention in the literature, as well as having significant implications for optimal protocol design.

We note several weaknesses in this study. Firstly, we concede that the lack of histological verification cannot formally exclude the possibility of benign causes of tracer uptake. Furthermore, without such confirmation, we cannot exclude the possibility of false positives. However, we note the multitude of studies confirming the high specificity of PSMA and we do not seek to duplicate these results, referring instead to the meta-analysis reported by Perera et al. [37]. Our small patient cohort did not lend itself to a subanalysis by the PSA group, for which further studies with larger cohorts are required. We also note that only one patient had a solid organ metastasis, and this study is therefore unable to answer how these lesions behave at late imaging. We also note that patients were investigated on one of the two scanner types, either a digital PET/CT (Siemens Biograph Vision-600) or one of the two cross-calibrated scanners (Siemens mCT-Biograph). Cognisant of the influence which reconstruction algorithm and scanner type plays on SUV [38], we restricted our analysis to a dimensionless ratio between late and standard imaging, and post hoc analysis revealed no significant influence of either scanner type or lesion size on tracer uptake behaviour. We also note that whilst, as argued above, additional late imaging has several advantages, it does entail an increase in the examination time and the additional radiation dose associated with a low-dose CT for attenuation correction.

Conclusion

In this first description of dynamic patterns of tracer uptake by lesion type, we find a heterogeneous pattern of tracer uptake for all lesion types, with no particular lesion type exhibiting uniformly increasing tracer uptake. The assumption, therefore, that all pathological PC lesions demonstrate increasing tracer uptake at late imaging is a potential diagnostic pitfall. Furthermore, the heterogeneity of lesion behaviour, in particular, the finding that nearly one in five bone lesions exhibited decreasing tracer uptake at late imaging potentially points towards an important difference in tumour biology for these lesion types, which, if confirmed by further studies, would have significant implications for PSMA radioligand therapy of PC.

Acknowledgements This thesis forms part of the doctorial thesis of I Alberts.

Compliance with ethical standards

Ethical approval All patients published in this manuscript signed a written informed consent form for the purpose of anonymised evaluation and the publication of their data. This evaluation was approved by the ethics committee of the University of Bern (KEK-Nr. 2018-00299).

Conflict of interest The authors declare that they have no conflict of interest.

References

1. Siegel RL, Miller KD, Jemal A. Cancer statistics, 2017. CA Cancer J Clin. 2017;67:7–30. https://doi.org/10.3322/caac.21387.
2. Fossati N, Karnes RJ, Colicchia M, Boorjian SA, Bossi A, Seisen T, et al. Impact of early salvage radiation therapy in patients with persistently elevated or rising prostate-specific antigen after radical prostatectomy. Eur Urol. 2017. https://doi.org/10.1016/j.eururo.2017.07.026.
3. Israeli RS, Powell CT, Corr JG, Fair WR, Heston WDW. Expression of the prostate-specific membrane antigen. Cancer Res. 1994;54:1807.
4. Afshar-Oromieh A, Zechmann CM, Malcher A, Eder M, Eisenhut M, Linhart HG, et al. Comparison of PET imaging with a (68)Ga-labelled PSMA ligand and (18)F-choline-based PET/CT for the diagnosis of recurrent prostate cancer. Eur J Nucl Med Mol Imaging. 2014;41:11–20. https://doi.org/10.1007/s00259-013-2525-5.
5. Afshar-Oromieh A, Holland-Letz T, Giesel FL, Kratochwil C, Mier W, Haufe S, et al. Diagnostic performance of 68Ga-PSMA-11 (HBED-CC) PET/CT in patients with recurrent prostate cancer: evaluation in 1007 patients. Eur J Nucl Med Mol Imaging. 2017;44:1258–68. https://doi.org/10.1007/s00259-017-3711-7.
6. Eiber M, Maurer T, Souvatzoglou M, Beer AJ, Ruffani A, Haller B, et al. Evaluation of hybrid (68)Ga-PSMA ligand PET/CT in 248 patients with biochemical recurrence after radical prostatectomy. J Nucl Med. 2015;56:668–74. https://doi.org/10.2967/jnumed.115.154153.
7. Afshar-Oromieh A, Avtzi E, Giesel FL, Holland-Letz T, Linhart HG, Eder M, et al. The diagnostic value of PET/CT imaging with the (68)Ga-labelled PSMA ligand HBED-CC in the diagnosis of recurrent prostate cancer. Eur J Nucl Med Mol Imaging. 2015;42:197–209. https://doi.org/10.1007/s00259-014-2949-6.
8. Virgolini I, Decristoforo C, Haug A, Fanti S, Uprimny C. Current status of theranostics in prostate cancer. Eur J Nucl Med Mol Imaging. 2018;45:471–95. https://doi.org/10.1007/s00259-017-3882-2.
9. Chang SS. Overview of prostate-specific membrane antigen. Rev Urol. 2004;6:S13–S8.
10. Afshar-Oromieh A, Malcher A, Eder M, Eisenhut M, Linhart HG, Hadaschik BA, et al. PET imaging with a [68Ga]gallium-labelled PSMA ligand for the diagnosis of prostate cancer: biodistribution in humans and first evaluation of tumour lesions. Eur J Nucl Med Mol Imaging. 2013;40:486–95. https://doi.org/10.1007/s00259-012-2298-2.
11. Afshar-Oromieh A, Sattler LP, Steiger K, Holland-Letz T, da Cunha ML, Mier W, et al. Tracer uptake in mediastinal and paraaortal thoracic lymph nodes as a potential pitfall in image interpretation

of PSMA ligand PET/CT. Eur J Nucl Med Mol Imaging. 2018;45:1179–87. https://doi.org/10.1007/s00259-018-3965-8.
12. Krohn T, Verburg FA, Pufe T, Neuhuber W, Vogg A, Heinzel A, et al. [(68)Ga]PSMA-HBED uptake mimicking lymph node metastasis in coeliac ganglia: an important pitfall in clinical practice. Eur J NuclMed Mol Imaging. 2015;42:210–4. https://doi.org/10.1007/s00259-014-2915-3.
13. Werner RA, Sheikhbahaei S, Jones KM, Javadi MS, Solnes LB, Ross AE, et al. Patterns of uptake of prostate-specific membrane antigen (PSMA)-targeted (18)F-DCFPyL in peripheral ganglia. Ann Nucl Med. 2017;31:696–702. https://doi.org/10.1007/s12149-017-1201-4.
14. Kanthan GL, Hsiao E, Vu D, Schembri GP. Uptake in sympathetic ganglia on 68Ga-PSMA-HBED PET/CT: a potential pitfall in scan interpretation. J Med Imaging Radiat Oncol. 2017;61:732–8. https://doi.org/10.1111/1754-9485.12622.
15. Hubble D, Robins P. RE: Uptake in sympathetic ganglia on 68Ga-PSMA-HBED PET/CT: a potential pitfall in scan interpretation. J Med Imaging Radiat Oncol. 2018;62:377–8. https://doi.org/10.1111/1754-9485.12739.
16. Rischpler C, Beck TI, Okamoto S, Schlitter AM, Knorr K, Schwaiger M, et al. (68)Ga-PSMA-HBED-CC uptake in cervical, coeliac and sacral ganglia as an important pitfall in prostate cancer PET imaging. J Nucl Med. 2018. https://doi.org/10.2967/jnumed.117.204677.
17. Afshar-Oromieh A, Sattler LP, Mier W, Hadaschik BA, Debus J, Holland-Letz T, et al. The clinical impact of additional late PET/CT imaging with (68)Ga-PSMA-11 (HBED-CC) in the diagnosis of prostate cancer. J Nucl Med. 2017;58:750–5. https://doi.org/10.2967/jnumed.116.183483.
18. Afshar-Oromieh A, Hetzheim H, Kubler W, Kratochwil C, Giesel FL, Hope TA, et al. Radiation dosimetry of (68)Ga-PSMA-11 (HBED-CC) and preliminary evaluation of optimal imaging timing. Eur J Nucl Med Mol Imaging. 2016;43:1611–20. https://doi.org/10.1007/s00259-016-3419-0.
19. Afshar-Oromieh A, Hetzheim H, Kratochwil C, Benesova M, Eder M, Neels OC, et al. The theranostic PSMA ligand PSMA-617 in the diagnosis of prostate cancer by PET/CT: biodistribution in humans, radiation dosimetry, and first evaluation of tumor lesions. J Nucl Med. 2015;56:1697–705. https://doi.org/10.2967/jnumed.115.161299.
20. Eder M, Neels O, Muller M, Bauder-Wust U, Remde Y, Schafer M, et al. Novel preclinical and radiopharmaceutical aspects of [68Ga]Ga-PSMA-HBED-CC: a new PET tracer for imaging of prostate cancer. Pharmaceuticals (Basel). 7:779–96. https://doi.org/10.3390/ph7070779.
21. Sachpekidis C, Baumer P, Kopka K, Hadaschik BA, Hohenfellner M, Kopp-Schneider A, et al. (68)Ga-PSMA PET/CT in the evaluation of bone metastases in prostate cancer. Eur J Nucl Med Mol Imaging. 2018;45:904–12. https://doi.org/10.1007/s00259-018-3936-0.
22. Lodge MA. Repeatability of SUV in oncologic (18)F-FDG PET. J Nucl Med. 2017;58:523–32. https://doi.org/10.2967/jnumed.116.186353.
23. Osborne JR, Kalidindi TM, Punzalan BJ, Gangangari K, Spratt DE, Weber WA, et al. Repeatability of [(68)Ga]DKFZ11-PSMA PET scans for detecting prostate-specific membrane antigen-positive prostate cancer. Mol Imaging Biol. 2017;19:944–51. https://doi.org/10.1007/s11307-017-1091-9.
24. Rahbar K, Afshar-Oromieh A, Seifert R, Wagner S, Schafers M, Bogemann M, et al. Diagnostic performance of (18)F-PSMA-1007 PET/CT in patients with biochemical recurrent prostate cancer. Eur J Nucl Med Mol Imaging. 2018;45:2055–61. https://doi.org/10.1007/s00259-018-4089-x.
25. Fendler WP, Eiber M, Beheshti M, Bomanji J, Ceci F, Cho S, et al. (68)Ga-PSMA PET/CT: Joint EANM and SNMMI procedure guideline for prostate cancer imaging: version 1.0. Eur J Nucl Med Mol Imaging. 2017;44:1014–24. https://doi.org/10.1007/s00259-017-3670-z.
26. Sahlmann C-O, Meller B, Bouter C, Ritter CO, Ströbel P, Lotz J, et al. Biphasic 68Ga-PSMA-HBED-CC-PET/CT in patients with recurrent and high-risk prostate carcinoma. Eur J Nucl Med Mol Imaging. 2016;43:898–905. https://doi.org/10.1007/s00259-015-3251-y.
27. Bialek EJ, Malkowski B. Celiac ganglia: can they be misinterpreted on multimodal 68Ga-PSMA-11 PET/MR? Nucl Med Commun. 2019;40:175–84. https://doi.org/10.1097/MNM.0000000000000944.
28. Schillaci O, Urbano N. Digital PET/CT: a new intriguing chance for clinical nuclear medicine and personalized molecular imaging. Eur J Nucl Med Mol Imaging. 2019. https://doi.org/10.1007/s00259-019-04300-z.
29. Giesel FL, Knorr K, Spohn F, Will L, Maurer T, Flechsig P, et al. Detection efficacy of (18)F-PSMA-1007 PET/CT in 251 patients with biochemical recurrence of prostate cancer after radical prostatectomy. J Nucl Med. 2019;60:362–8. https://doi.org/10.2967/jnumed.118.212233.
30. Fendler WP, Calais J, Eiber M, Flavell RR, Mishoe A, Feng FY, et al. Assessment of 68Ga-PSMA-11 PET accuracy in localizing recurrent prostate cancer: a prospective single-arm clinical trial. JAMA Oncol. 2019. https://doi.org/10.1001/jamaoncol.2019.0096.
31. Woythal N, Arsenic R, Kempkensteffen C, Miller K, Janssen JC, Huang K, et al. Immunohistochemical validation of PSMA expression measured by (68)Ga-PSMA PET/CT in primary prostate cancer. J Nucl Med. 2018;59:238–43. https://doi.org/10.2967/jnumed.117.195172.
32. Sachpekidis C, Kopka K, Eder M, Hadaschik BA, Freitag MT, Pan L, et al. 68Ga-PSMA-11 dynamic PET/CT imaging in primary prostate cancer. Clin Nucl Med. 2016;41:e473–e9. https://doi.org/10.1097/RLU.0000000000001349.
33. Rajasekaran SA, Anilkumar G, Oshima E, Bowie JU, Liu H, Heston W, et al. A novel cytoplasmic tail MXXXL motif mediates the internalization of prostate-specific membrane antigen. Mol Biol Cell. 2003;14:4835–45. https://doi.org/10.1091/mbc.e02-11-0731.
34. Budäus L, Leyh-Bannurah S-R, Salomon G, Michl U, Heinzer H, Huland H, et al. Initial experience of 68Ga-PSMA PET/CT imaging in high-risk prostate cancer patients prior to radical prostatectomy. Eur Urol. 2016;69:393–6. https://doi.org/10.1016/j.eururo.2015.06.010.
35. Wieser G, Popp I, Christian Rischke H, Drendel V, Grosu AL, Bartholoma M, et al. Diagnosis of recurrent prostate cancer with PET/CT imaging using the gastrin-releasing peptide receptor antagonist (68)Ga-RM2: preliminary results in patients with negative or inconclusive [(18)F]Fluoroethylcholine-PET/CT. Eur J Nucl Med Mol Imaging. 2017;44:1463–72. https://doi.org/10.1007/s00259-017-3702-8.
36. EANM'15, 28th Annual EANM Congress of the European Association of Nuclear Medicine 2015, 10-14 October 2015, Hamburg, Germany. European journal of nuclear medicine and molecular imaging. 2015;42 Suppl 1:S1-924. https://doi.org/10.1007/s00259-015-3198-z.
37. Perera M, Papa N, Christidis D, Wetherell D, Hofman MS, Murphy DG, et al. Sensitivity, specificity, and predictors of positive (68)Ga-prostate-specific membrane antigen positron emission tomography in advanced prostate cancer: a systematic review and meta-analysis. Eur Urol. 2016;70:926–37. https://doi.org/10.1016/j.eururo.2016.06.021.
38. van Sluis JJ, de Jong J, Schaar J, Noordzij W, van Snick P, Dierckx R, et al. Performance characteristics of the digital Biograph Vision PET/CT system. J Nucl Med. 2019. https://doi.org/10.2967/jnumed.118.215418.